Co-published by
Institute of Fluid-Flow Machinery
Polish Academy of Sciences
Committee on Thermodynamics and Combustion
Polish Academy of Sciences

http://www.imp.gda.pl/archives-of-thermodynamics/

Analysis of entropy generation in unsteady flow of nanofluids past a convectively heated moving permeable cylindrical surface

Itumeleng Chokoe[a*], Oluwole Daniel Makinde[a], Ramotjaki Lucky Monaledi[a]

[a] Stellenbosch University, Faculty of Military Science, Private Bag X2, Saldanha, 7395, South Africa
*Corresponding author email: igchokoe21@gmail.com

Received: 12.10.2023; revised: 05.02.2024; accepted: 08.04.2024

Abstract

This paper investigates entropy generation rate in a temperature-dependent variable viscosity unsteady nanofluid flow past a convectively heated impulsively moving permeable cylindrical surface. The governing equations based on the modified Stokes first problem assumption are obtained and transformed using appropriate similarity variables into nonlinear ordinary differential equations. The numerical shooting method together with the Runge-Kutta Fehlberg integration scheme are employed to effectively solve the problem. The effects of related parameters on the nanofluid velocity, temperature, skin friction, Nusselt number, entropy generation rate and Bejan number are displayed graphically and quantitatively explained. It is found that an upsurge in nanoparticles volume fraction enhances the skin friction, Nusselt number, entropy production rate and the Bejan number.

Keywords: Entropy generation; Unsteady nanofluid flow; Permeable cylindrical surface; Numerical shooting method

Vol. 45(2024), No. 3, 107–113; doi: 10.24425/ather.2024.151221

Cite this manuscript as: Chokoe, I., Makinde, O.D., & Monaledi, R.L. (2024). Analysis of entropy generation in unsteady flow of nanofluids past a convectively heated moving permeable cylindrical surface. *Archives of Thermodynamics*, 45(3), 107–113.

1. Introduction

Impulsively moving permeable heated cylindrical surface in an infinite nanofluid medium has a wide range of applications in engineering and industries. Such applications can be found in the production of composite substances, rocket launching, torpedo, missile, fired bullet, the processing of porous materials, submarine, thermal insulation, fuel production, glass processing, and thermal solar panels. Theoretically speaking, this problem is closely related to an extension of Stokes first problem of unsteady boundary layer flow past a moving cylindrical surface, as discussed by Stokes [1]. Meanwhile, Choi [2] coined the term nanofluid to describe the engineered colloidal suspension of nanometer-sized particles in a base fluid. The novelty of nanofluids lies in their heat transfer enhancement capability. Consequently, studies related to the boundary layer flow of nanofluid past a moving surface have attracted global attention due to their useful applications in many industrial and engineering sectors, as highlighted by Kuznetsov and Nield [3] and others [4–7].

In addition, the generation of entropy is also important in ensuring the effective functioning of fluid flow and thermal systems. This concept takes into account the depletion of useful energy within the system, as explained by Bejan [8]. Therefore, reducing the entropy generation rate is important in optimizing

Nomenclature

Be – Bejan number $\left(\mathrm{Be} = \frac{1}{1+\frac{N_2}{N_1}}\right)$

Bi – thermal Biot number $\left(\mathrm{Bi} = \frac{h_f\sqrt{\nu_f t}}{k_f}\right)$

C_f – skin friction

C_p – specific heat at constant pressure, J/(kg s)

Ec – Eckert number

E_g – volumetric entropy generation

h – heat transfer coefficient, W/(m^{2}K)

k – fluid thermal conductivity, W/(m K)

N_1 – irreversibility because of heat transfer

N_2 – entropy generation because of viscous dissipation

N_s – dimensionless entropy production rate

Nu– Nusselt number $\left(\mathrm{Nu} = \frac{a(t)q_w}{k_f(T_f - T_\infty)}\right)$

Pr – Prandtl number $\left(\mathrm{Pr} = \frac{\mu_f C_{pf}}{k_f}\right)$

T – fluid temperature, K

Greek symbols

β – variable viscosity parameter

η – dimensionless gap between two-cylinder

θ – dimensionless temperature

λ – horizontal movement parameter

μ – fluid dynamic viscosity (ambient temperature), kg/(m s)

ρ – density of the fluid, kg/m^3

Abbreviations and Acronyms

ODE – ordinary differential equation

IVP – initial value problem

MHD – magnetohydrodynamic

the thermodynamic performance of many engineering flow processes. Woods [9] states that the first law of thermodynamics is essentially a statement about the conservation of energy, while the second law of thermodynamics highlights how entropy generation makes technological processes irreversible. Theoretical studies on the second law analysis of fluid flow with heat transfer characteristics was pioneered by Bejan [10]. Butt et al. [11] examined the impact of entropy generation on a boundary layer flow and heat transfer of nanofluid over a cylindrical surface. Rana and Shukla [12] analytically investigated the effects of entropy production on hydromagnetic boundary layer flow of nanofluid past a flat plate with aligned magnetic fields, ohmic heating and viscous dissipation. Freidoonimehr and Rahimi [13] reported an exact solution for hydromagnetic nanofluid flow and heat transfer with entropy generation past a permeable stretching/shrinking sheet surface. The problem of inherent irreversibility in nanofluid flow over a convectively heated radially stretching disk was numerically examined by Das et al. [14]. Khan et al [15], explored the theoretical analysis for thermal and mass transport of Maxwell nanofluid along permeable shrinking surface. The results showed that the thermal boundary layer thickness decreases with stronger suction influence, resulting in an increase in heat and mass transfer rate. Zahmatkesh et al. [16] analyzed the effects of entropy generation rate on stagnation point flow of nanofluid towards a permeable cylindrical surface with uniform surface suction and injection. Muhammad and Makinde [17] discussed the thermodynamics irreversibility in an unsteady hydromagnetic mixed convective flow over a porous vertical surface under the combined impact of thermal radiation and velocity slip. Das et al. [18] numerically investigated the unsteady hydromagnetic boundary layer flow and heat transfer of nanofluid past an impulsive convectively heated stretching sheet with heat source/sink. The entropy generation and heat transfer of dissipative mixed convection of nanofluid over a vertical cylindrical surface was explored by Agrawal and Kaswan [19]. Kumar and Mondal [20] studied the flow of heat-radiating hybrid nanofluids through a stretchable rotating disk with entropy generation in the presence of a magnetic field. The effects of entropy generation rate on MHD boundary layer flow of a radiating carbon nano-tubes nanofluid was numerically investigated by Mandal and Pal [21].

The aim of this study is to investigate the rate at which entropy is produced in a flow of nanofluids with temperature-dependent viscosity past a permeable cylindrical surface that is heated and moves impulsively in both vertical and horizontal directions. This research focused on using copper as nanoparticles and water as the base fluid. Previous research has not explored this particular geometry, so this study aims to fill that gap in the literature. Moreover, the inclusion of viscous and porous dissipation terms in the energy equation enables us to examine their effect on fluid flow and heat transfer. The relevant equations governing the system are derived and transformed into ordinary differential equations using appropriate similarity variables. To solve the model problem, a numerical procedure called shooting method is employed, which reformulates the original boundary value problem to a related initial value problem (IVPs) with its appropriate initial conditions, presented by Ha [22]. The resultant IVP is solved numerically using the Runge-Kutta-Fehlberg integration scheme method for solving linear ordinary differential equations. The results obtained show the impact of various parameters on velocity, temperature, skin friction, Nusselt number, entropy generation rate, and Bejan number. These results are presented graphically and discussed in detail.

2. Model problem

Consider an unsteady flow of a variable viscosity Cu-water nanofluid generated by the impulsive motion of a convectively heated permeable cylindrical surface. It is assumed that the cylindrical body is subjected to both horizontal and vertical motion as shown in Fig. 1 below.

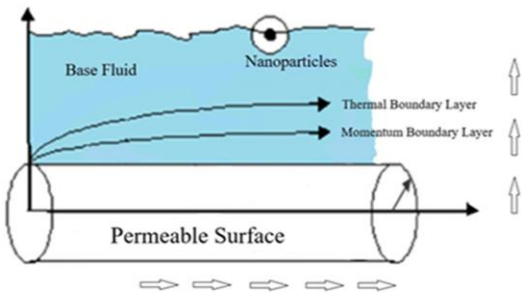

Fig. 1. Geometry of the problem.

The equations that govern the flow field in the boundary layer are based on the above assumptions, the conservation of mass, momentum, energy and entropy generation. Using the boundary layer approximation, as discussed by Munawar et al. [23], the governing equations of continuity, momentum, energy and entropy generation rate in cylindrical coordinates, may be written in the usual notation as [6,16,19,23]:

$$\frac{\partial u}{\partial z} = -\frac{V}{r}, \tag{1}$$

$$\frac{\partial u}{\partial t} + V\left(\frac{\partial u}{\partial r} - \frac{u}{r}\right) = \frac{1}{\rho_{nf} r}\frac{\partial}{\partial r}\left(r\mu_{nf}\frac{\partial u}{\partial r}\right), \tag{2}$$

$$\frac{\partial T}{\partial t} + V\frac{\partial T}{\partial r} = \frac{k_{nf}}{(\rho C_p)_{nf}}\frac{1}{r}\frac{\partial}{\partial r}\left(r\frac{\partial T}{\partial r}\right) + \frac{\mu_{nf}}{(\rho C_p)_{nf}}\left(\frac{\partial u}{\partial r}\right)^2, \tag{3}$$

$$E_g = \frac{k_{nf}}{(T_f - T_\infty)^2}\left(\frac{\partial T}{\partial r}\right)^2 + \frac{\mu_{nf}}{(T_f - T_\infty)}\left(\frac{\partial u}{\partial r}\right)^2, \tag{4}$$

subjected to the boundary conditions

– at $r = a(t)$:

$$u(a,t) = U_0,\ -k_f\frac{\partial T}{\partial r}(a,t) = h_f\left[T_f - T(a,t)\right], \tag{5a}$$

– as $r \to \infty$: $\quad u(\infty,t) \to U_\infty, \quad T(\infty,t) \to T_\infty,$ (5b)

where u is the velocity in the z-direction while V is the velocity in the r-direction of the cylindrical polar coordinates, r is the radius of the cylinder, z is the axial distance, t is the time, U_∞ is the free stream velocity, U_0 is the velocity of cylindrical surface impulsive motion, μ_{nf} – the nanofluid dynamic viscosity, ρ_{nf} – the nanofluid density, T is the temperature, k_{nf} is the conductivity of the nanofluid, $(\rho C_p)_{nf}$ – the specific heat capacitance of nanofluid, T_f is the hot fluid temperature at the surface, T_∞ is the free stream temperature, k_f – thermal conductivity of the base fluid, and h_f is the heat transfer coefficient. The physical properties of water together with copper nanoparticles are listed in Table 1 below.

Table 1. Nanoparticles and base fluid thermophysical properties [25,26].

Materials	ρ [kg/m³]	C_p [J/(kgK)]	k [W/(mK)]
Pure water	997.1	4179	0.613
Copper (Cu)	8933	385	401

2.1. Similarity transformation

The system of differential Equations (1)–(5) consists of coupled nonlinear equations. Specific feasible similarity transformations can be utilized to transform the nonlinear system of partial differential equations into a nonlinear system of ordinary differential equations to achieve such simplifications. The following similarity variables are taken into consideration:

$$\eta = \frac{r}{\sqrt{\nu_f t}} - s, \quad V = -c\sqrt{\frac{\nu_f}{t}}, \quad \theta(\xi) = \frac{T - T_\infty}{(T_f - T_\infty)}, \quad u = U_\infty F(\eta), \tag{6}$$

$$\beta = M\left(T_f - T_\infty\right), \quad \mu_{nf} = \frac{\mu_f e^{-M\left(T_f - T_\infty\right)}}{(1-\phi)^{2.5}}, \quad a(t) = s\sqrt{\nu_f t}\,.$$

By substituting Eq. (6) into Eqs. (1)–(5) we obtain the dimensionless ordinary differential equations:

$$F'' + \left[\frac{1}{\eta+s} - \beta\theta' + A_1A_2e^{\beta\theta}\left(\frac{(\eta+s)}{2} + c\right)\right]F' - \frac{cA_1A_2}{\eta+s}e^{\beta\theta}F = 0, \tag{7}$$

$$\theta'' + \left[\frac{1}{\eta+s} + \mathrm{Pr}A_4A_5\left(\frac{\eta+s}{2} + c\right)\right]\theta' + A_3A_4\mathrm{PrEc}e^{-\beta\theta}(F')^2 = 0, \tag{8}$$

$$N_s = \left(\frac{k_{nf}}{k_f}\right)(\theta')^2 + \frac{\mathrm{PrEc}e^{-\beta\theta}}{(1-\phi)^{2.5}}(F')^2 = 0, \tag{9}$$

subjected to the boundary conditions:

$$F(0) = \lambda, \qquad \theta'(0) = -\mathrm{Bi}\left(1 - \theta(0)\right),$$
$$F(\infty) = 1, \qquad \theta(\infty) = 0. \tag{10}$$

The dimensionless parameters are defined as:

$$A_1 = \frac{\rho_{nf}}{\rho_f}, \quad A_2 = (1-\phi)^{2.5}, \quad A_3 = (1-\phi)^{-2.5},$$
$$A_4 = \frac{k_f}{k_{nf}}, \quad A_5 = \frac{(\rho C_p)_{nf}}{(\rho C_p)_f}, \quad \lambda = \frac{U_0}{U_\infty}, \tag{11}$$
$$\mathrm{Pr} = \frac{\mu_f C_{pf}}{k_f}, \quad \mathrm{Bi} = \frac{h_f\sqrt{\nu_f t}}{k_f}, \quad \mathrm{Ec} = \frac{U_\infty^2}{(C_p)_f(T_f - T_\infty)}.$$

The physical parameters of interest influencing the flow system are ϕ which represents the nanofluid volume fraction, β representing the variable viscosity parameter of the nanofluid, s representing the vertical movement of the cylindrical surface; Pr is the base fluid Prandtl number (Pr = 6.2), which is a ratio of momentum diffusivity to thermal diffusivity, Ec is the Eckert number that defines a ratio of the advective mass transfer to the heat dissipation, λ is the horizontal movement of the model, $c > 0$ represents nanofluid suction and $c < 0$ is the nanofluid injection, N_s is the dimensionless entropy generation rate and Bi is the Biot number defined as the ratio of thermal resistance between the body and the surface of the body.

Other interesting engineering quantities are the coefficient of skin friction C_f, the Nusselt number Nu and the Bejan number Be, given by the following equations:

$$\mathrm{Re}_t C_f = \frac{e^{-\beta\theta(0)}F'(0)}{(1-\phi)^{2.5}}, \quad \mathrm{Nu} = -s\frac{k_{nf}}{k_f}\theta'(0), \quad \mathrm{Be} = \frac{1}{1+\Phi}, \tag{12}$$

where:

$$C_f = \frac{\tau_w}{\rho_f U_\infty^2}, \quad \mathrm{Nu} = \frac{a(t)q_w}{k_f(T_f - T_\infty)}, \quad \tau_w = \mu_{nf}\frac{\partial u}{\partial r}\Big|_{r=a(t)},$$
$$q_w = -k_{nf}\frac{\partial T}{\partial r}\Big|_{r=a(t)}, \quad \mathrm{Re}_t = \frac{U_\infty\sqrt{\nu_f t}}{\nu_f}, \tag{13}$$
$$N_1 = \left(\frac{k_{nf}}{k_f}\right)(\theta')^2, \quad N_2 = \frac{\mathrm{PrEc}e^{-\beta\theta}}{(1-\phi)^{2.5}}(F')^2, \quad \Phi = \frac{N_2}{N_1},$$

and N_1 is the heat transfer irreversibility (HTI), N_2 is the fluid friction irreversibility (FFI), Φ is the irreversibility ratio, τ_w is the cylindrical surface shear stress, q_w is the dimensional heat flux, Re_t is the local Reynolds number.

For a constant viscosity convectional fluid flow past an impermeable stationary cylindrical surface, $\beta = c = \phi = \lambda = 0$ and $s = 1$. The model Eq. (7) is amenable to exact solution based on the boundary conditions in Eq. (10) and we obtain:

$$F(\eta) = \frac{E_i\left(\frac{(y+1)^2}{4}\right) - E_i\left(1,\ \frac{1}{4}\right)}{E_i\left(\frac{(\infty+1)^2}{4}\right) - E_i\left(1,\ \frac{1}{4}\right)}. \quad (14)$$

3. Numerical procedure

The shooting technique with the Runge-Kutta-Fehlberg integral scheme is a numerical method used to solve model equations. The dimensionless boundary value problem in the resulting Eqs. (7)–(8), is converted into an initial value problem (IVP) by letting:

$$x_1 = F(\eta), \quad x_2 = F'(\eta), \quad x_3 = \theta(\eta), \quad x_4 = \theta'(\eta) \quad (15)$$

and obtaining:

$$x_1{}' = x_2 \quad (16)$$

$$x_2{}' = \frac{cA_1A_2}{\eta+s} e^{\beta x_3} x_1 - \left[\frac{1}{\eta+S} - \beta x_4 + A_1A_2 e^{\beta x_3}\left(\frac{(\eta+s)}{2} + c\right)\right] x_2, \quad (17)$$

$$x_3{}' = x_4 \quad (18)$$

$$x_4{}' = -\left[\frac{1}{\eta+s} + P_r A_4 A_5\left(\frac{\eta+s}{2} + c\right)\right] x_4 - A_3A_4P_rE_c e^{-\beta x_3}(x_2)^2, \quad (19)$$

with the initial conditions:

$$x_1(0) = \lambda, \qquad x_2(0) = a_1, \quad (20a)$$

$$x_3(0) = a_2, \ x_4(0) = -Bi(1 - a_2). \quad (20b)$$

The initial values of a_1 and a_2 are guessed initially and successively obtained using the Newton-Raphson method. The numerical value is estimated using the shooting procedure. If these boundary conditions are not satisfied to the required accuracy, the procedure is repeated with a new set of initial conditions until the required accuracy is acquired or a limit to the iteration is reached [23]. The resultant IVP is solved numerically using any appropriate method for solving nonlinear ordinary differential equations (ODE). Then the subsequent system of a set of nonlinear ODEs is solved by using the Runge-Kutta-Fehlberg integration scheme.

4. Results and discussion

To fully understand the heat and mass transfer properties in the overall flow structure, numerical solutions showing the effect of emerging thermophysical parameters on the nanofluids, temperature profile, velocity profiles, skin friction, Nusselt number, entropy generation, and Bejan number are discussed, and graphically displayed in Figs. 2 to 15. To validate the accuracy of our numerical procedure, the numerical results obtained for velocity profiles are compared with their corresponding exact solutions displayed in Eq. (14). A very excellent agreement is achieved as depicted in Table 2. This undoubtedly attests to the accuracy of our numerical procedure and the obtained results. Table 2 presents a comparison between the exact and numerical results when $\beta = c = \phi = \lambda = 0$ and $s = 1$.

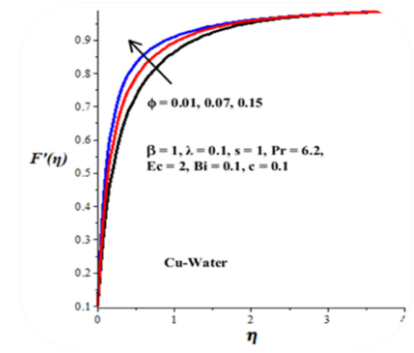

Fig. 2. The impact ϕ of on the velocity profile of Cu-water.

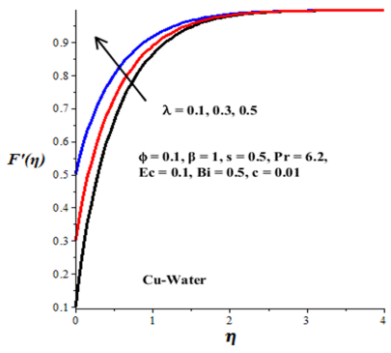

Fig. 3. The impact of λ on the velocity profile of Cu-water.

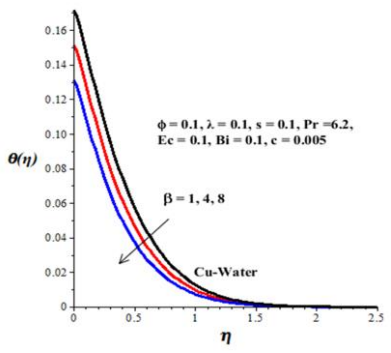

Fig. 4. The impact of β on the temperature profile of Cu-water.

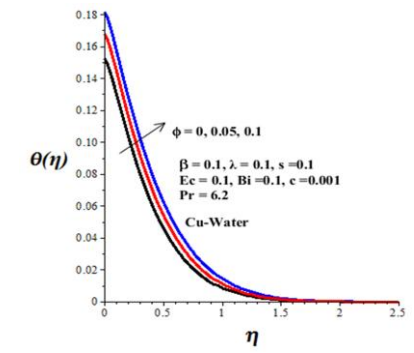

Fig. 5. The impact of ϕ on the temperature profile of Cu-water.

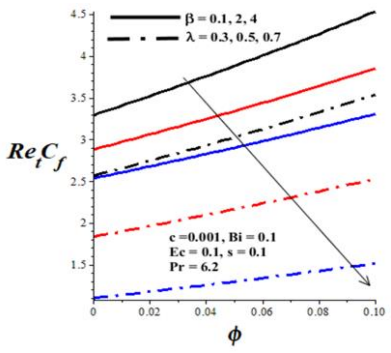

Fig. 6. The impact of ϕ, β and λ on the skin friction of Cu-water.

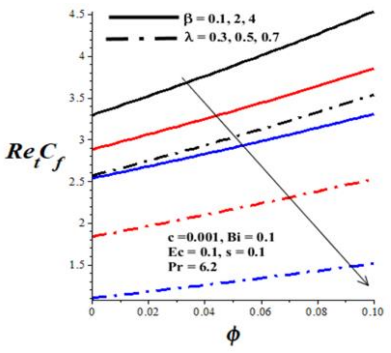

Fig. 7. The impact of s and c on the skin friction of Cu-water.

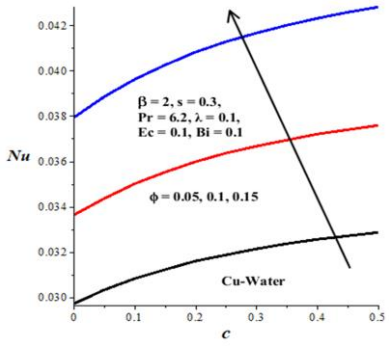

Fig. 8. The impact of ϕ with increase in c on the Nusselt number of Cu-water.

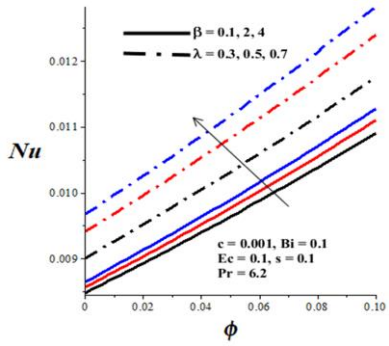

Fig. 9. The impact of β and λ with increase in ϕ on the Nusselt number of Cu-water

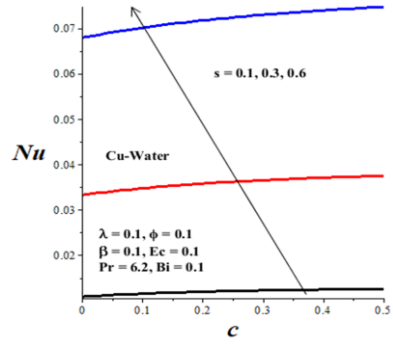

Fig. 10. The impact of s and c on the Nusselt number of Cu-water.

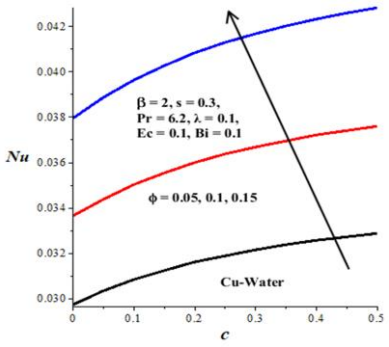

Fig. 11. The impact of ϕ and Ec on the entropy generation of Cu-water.

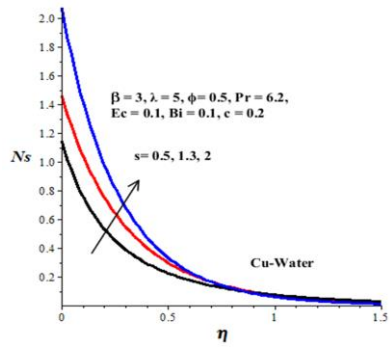

Fig. 12. The impact of s on the entropy generation of Cu-water.

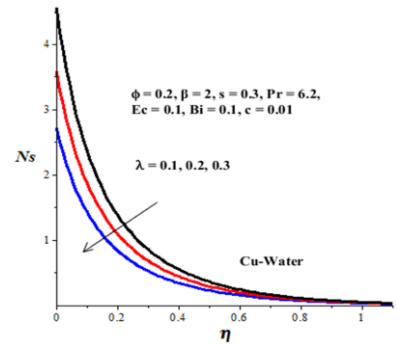

Fig. 13. The impact of λ on the entropy generation of Cu-water.

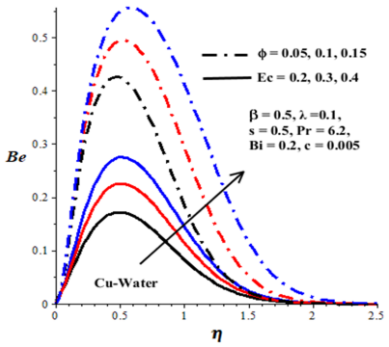

Fig. 14. The impact of ϕ and Ec on the Bejan number of Cu-water.

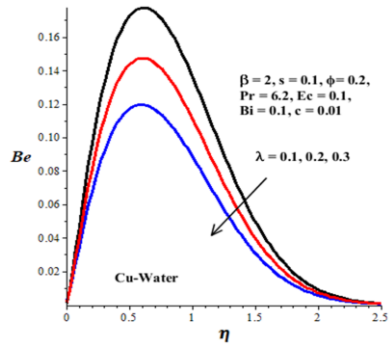

Fig. 15. The impact of λ on the Bejan number of Cu-water.

Table 1. Comparison between the exact and numerical results when $\beta = c = \phi = \lambda = 0$ and $s = 1$.

η	$F(\eta)$, Exact	$F(\eta)$, Numerical
0	0.00000000	0.00000000
0.1	0.13860827	0.13860830
0.3	0.36214317	0.36214315
0.6	0.59814367	0.59814374
1.0	0.78991900	0.78991910
2.0	0.96671207	0.96671210
4.0	0.99974099	0.99974100
∞	1.00000000	1.00000000

For this study, we used Cu-water nanofluid because of its high thermal conductivity. It can be observed from Fig. 2 that there is a decrease in the velocity boundary layer thickness with an increase in ϕ (nanoparticle volume fraction), this may be attributed to a slight increase in the base fluid viscosity due to the presence of nanoparticles. This improves the relationship between Cu-water nanofluid and the heated cylindrical surface resulting in the heat transfer rate enhancement. A similar trend is observed with the rise in the parameter values of λ (surface horizontal motion parameter). As the parameter λ rises, the velocity boundary layer thickness diminished, as a result, the interaction between the nanofluid and the heated cylindrical surface increases as depicted in Fig. 3. Figures 4–5 show the parameter effects on nanofluid thermal boundary layer thickness. A decline in thermal boundary layer thickness and nanofluid temperature are observed with an upsurge in β (variable viscosity parameter). This can be observed by considering Eq. (6), as β increases the viscosity of the nanofluid reduces causing the fluid to be less dense affecting the heat transfer rate of the system (see Fig. 4). In Fig. 5, the temperature profile shows that the temperature of the nanofluid is maximized on the cylindrical surface by heat convection, improving heat transfer and decreasing at a moderate rate towards the free flow temperature far from the surface,

hence an increase in the value of ϕ (nanoparticle volume fraction) escalates the thermal boundary layer thickness.

Figures 6–7 show the parameter effects on skin friction between the nanofluid and the heated surface. It's observed that skin friction lessened with an upsurge in β (variable viscosity parameter) and λ (surface horizontal motion parameter). This is evident that when the value of β amplifies, the nanofluid viscosity is lightened reducing the friction caused by the copper nanoparticle on the cylindrical surface. However, with a rise in the value of ϕ (nanoparticle volume fraction), the skin friction intensifies due to the increasing presence of copper nanoparticles in the base fluid as illustrated in Fig. 6. In Fig. 7, a decline in skin friction is observed with elevated values of s (surface vertical motion parameter) and c (nanofluid suction at the surface). The effects of parameters on the Nusselt number which represents the rate at which heat is transferred from the heated surface to the nanofluid are shown in Figs. 8–10. The heat transfer rate is enhanced with an upsurge in the parameter value of ϕ and c due to elevation in temperature gradient at the surface (see Fig. 8). Similar results are observed in Figs. 9–10 with the rise in β, λ and s. The impact on the entropy generation rate by various parameters is depicted in Figs. 11–13. In general, the entropy generation rate attained its maximum value at the heated cylindrical surface and steadily reduces to the value of zero far away from the heated surface at the free stream region. However, the entropy generation rate is enhanced with an upsurge in parameter values of ϕ, Ec and s (see Figs. 11–12) but lessened with a rise in parameter value of λ (see Fig. 13).

This implies that an intensification in the number of nanoparticles in the base fluid coupled with the vertical motion of the surface may boost the entropy production in the flow process, consequently, lessening the flow efficiency. Figures 14–15 illustrate the parameter effects on the Bejan number which is the ratio of heat transfer irreversibility to the total entropy production in the flow system. Generally, it is observed that the Bejan number is minimum with zero value both at the cylindrical heated surface and the free stream region, however, within the boundary layer region the maximum value of the Bejan number is achieved. This simply implies that only fluid friction irreversibility contributes to the entropy production rate both at the heated surface and free stream region while the effects of both heat transfer and fluid friction irreversibilities are heightened within the boundary layer region. It is fascinating to mention that an increase in ϕ and Ec enhances the impact of heat transfer irreversibility in the flow process (Fig. 14) while an increase in λ lessened the impact of heat transfer irreversibility as depicted in Fig. 15.

5. Conclusions

The inherent irreversibility in unsteady nanofluid flow past a convectively heated impulsively moving permeable cylindrical surface has been investigated. The governing nonlinear differential equations based on modified Stoke's first problem assumption were obtained and numerically examined via the shooting method coupled with the Runge-Kutta-Fehlberg integration scheme. The main results can be summarized as follows:

- The velocity boundary layer thickness is reduced with an upsurge in the nanoparticle's volume fraction and surface horizontal motion.
- The thermal boundary layer thickness diminished with a decrease in nanofluid viscosity but amplified with increasing nanoparticle volume fraction.
- The skin friction reduces with a rise in variable viscosity parameter, surface horizontal motion parameter, surface vertical motion parameter and nanofluid suction at the surface but escalates with a rise in nanoparticle volume fraction.
- The Nusselt number is enhanced with elevated values of nanoparticle volume fraction, variable viscosity parameter, nanofluid suction, horizontal and vertical motion parameters.
- Maximum entropy production occurred at the heated cylindrical surface while the minimum was observed at the free stream region. An increase in nanoparticle volume fraction, Eckert number and surface vertical motion strengthens the entropy generation rate while a rise in horizontal motion lessened it.
- The Bejan number at both the heated surface and free stream is zero, consequently, only fluid friction irreversibility ensued. Within the boundary layer region, both heat transfer irreversibility and fluid friction irreversibility occurred with Be > 0. The Bejan number is enhanced with a rise in nanoparticle volume fraction and Eckert number but lessened with the heated surface horizontal motion.

In conclusion, entropy generation minimization is an essential factor for the efficient performance of a nanofluid thermal boundary layer flow system. This can be achieved by appropriately regulating the values of the emerging thermophysical parameters in the system. This will innovatively boost the coolant effectiveness in various engineering and industrial applications. It is observed that there are strong interdependencies of the flow variables on entropy generation, and the investigation has potential utilizations in the thermal management and energy conversion systems. For future research, concepts such as magneto-hydrodynamic and concentration can be included to better modify the current model.

Acknowledgements

The authors appreciate the constructive improvement suggestions of the anonymous reviewers. This work is based on the research supported wholly/in part by the National Research Foundation of South Africa (Grant Numbers 150670).

References

[1] Stokes, G.G. (1851). On the effect of the internal friction of fluids on the motion of pendulums. *Transactions of the Cambridge Philosophical Society, Part II*, 9, 8–106. doi: 10.4236/ojapps.2014.43010

[2] Choi, S.U.S. (1995). Enhancing thermal conductivity of fluids with nanoparticles. *American Society of Mechanical Engineers. Fluids Engineering Division*, 66, 99–105.

[3] Kuznetsov, A.V., & Nield, D.A. (2010). Natural convection boundary layer flow of a nanofluid past a vertical plate. *International Journal of Thermal Sciences*, 49, 243–247. doi: 10.1016/j.ijthermalsci.2013.10.007

[4] Khan, W.A., & Pop, I. (2010). Boundary-layer flow of a nanofluid past a stretching sheet. *International Journal of Heat and Mass Transfer*, 53(11), 2477–2483. doi: 10.1016/j.ijheatmasstransfer.2010.01.032

[5] Abbas, Z., & Sheikh, M. (2017). Numerical study of homogeneous–heterogeneous reactions on stagnation point flow of ferrofluid with non-linear slip condition. *Chinese Journal of Chemical Engineering*, 25(1), 11–17. doi: 10.1016/j.cjche.2016.05.019

[6] Makinde, O.D., Khan, W., & Khan, Z. (2017). Stagnation point flow of MHD chemically reacting nanofluid over a stretching convective surface with slip and radiative heat. *Part E: Journal of Process Mechanical Engineering*, 231(4), 695–703. doi: 10.1177/0954408916629506

[7] Rashidi, M., Ganesh, N.V., Hakeem, A.A., & Ganga, B. (2014). Buoyancy effect on MHD flow of nanofluid over a stretching sheet in the presence of thermal radiation. *Journal of Molecular Liquids*, 198, 234–238. doi: 10.1016/j.molliq.2014.06.037

[8] Bejan, A. (1996). *Entropy Generation Minimization*. CRC Press: New York, NY, USA.

[9] Woods, L.C. (1975). *The Thermodynamics of Fluid Systems*. Oxford University Press: Oxford, UK.

[10] Bejan, A. (1980). Second law analysis in heat transfer. *Energy*, 5(8–9), 720–732. doi: 10.1016/0360-5442(80)90091-2

[11] Butt, A.S., Tufail, M.N., Ali, A., & Dar, A. (2019). Theoretical investigation of entropy generation effects in nanofluid flow over an inclined stretching cylinder. *International Journal of Exergy*, 28(2), 126–157. doi: 10.1504/IJEX.2019.097976

[12] Rana, P., & Shukla, N. (2018). Entropy generation analysis for non-similar analytical study of nanofluid flow and heat transfer under the influence of aligned magnetic field. *Alexandria Engineering Journal*, 57, 3299–3310. doi: 10.1016/j.aej.2017.12.007

[13] Freidoonimehr, F., & Rahimi, A.B. (2017). Exact solution of entropy generation for MHD nanofluid flow induced by a stretching/shrinking sheet with transpiration: dual solution. *Advances in Powder Technology*, 28(2), 671–685. doi: 10.1016/j.apt.2016.12.005

[14] Das, S., Chakraborty, S., Jana, R.N., & Makinde, O.D. (2016). Entropy analysis of nanofluid flow over a convectively heated radially stretching disk embedded in a porous medium. *Journal of Nanofluids*, 5(1), 48–58. doi: 10.1166/jon.2016.1184

[15] Khan, M.N., Ullah, N., & Nadeem, S. (2021). Transient flow of Maxwell Nanofluid Over a Shrinking Surface: Numerical Solutions and Stability Analysis. *Surfaces and Interfaces*, 22, 100829. doi: 10.1016/j.surfin.2020.100829

[16] Zahmatkesh, R., Mohammadiun, H., Mohammadiun, M., & Dibaei-Bonab, M.H. (2019). Investigation of entropy generation in nanofluid's axisymmetric stagnation flow over a cylinder with constant wall temperature and uniform surface suction-blowing. *Alexandria Engineering Journal*, 58, 1483–1498. doi: 10.1016/j.aej.2019.12.003

[17] Muhammad, A., & Makinde, O.D. (2019). Thermodynamics analysis of unsteady MHD mixed convection with slip and thermal radiation over a permeable surface. *Defect and Diffusion Forum*, 374, 29–46. doi: 10.4028/www.scientific.net/DDF.374.29

[18] Das, S., Chakraborty, S., Jana, R.N., & Makinde, O.D. (2015). Entropy analysis of unsteady magneto-nanofluid flow past accelerating stretching sheet with convective boundary condition. *Applied Mathematics and Mechanics*, 36(12), 1593–1610. doi: 10.1007/s10483-015-2003-6

[19] Agrawal, R., & Kaswan, P. (2022). Minimization of the entropy generation in MHD flow and heat transfer of nanofluid over a vertical cylinder under the influence of thermal radiation and slip condition. *Heat Transfer*, 51, 1790–1808. doi: 10.1002/htj.22375

[20] Kumar, M., & Mondal, P.K. (2022). Irreversibility analysis of hybrid nanofluid flow over a rotating disk: Effect of thermal radiation and magnetic field. *Colloids and Surfaces A: Physicochemical and Engineering Aspects*, 635, 128077. doi: 10.1016/j.colsurfa.2021.128077

[21] Mandal, G., & Pal, D. (2021). Entropy generation analysis of radiated magnetohydrodynamic flow of carbon nanotubes nanofluids with variable conductivity and diffusivity subjected to chemical reaction. *Journal of Nanofluids*, 10, 491–505. doi: 10.1166/jon.2021.1812

[22] Ha, S.N. (2001). A nonlinear shooting method for two-point boundary value problems. *International Journal of Computers and Mathematics with Applications*, 42(10), 1411–1420. doi: 10.1016/S0898-1221(01)00250-4

[23] Munawar, S., Saleem, N., & Mehmood, A. (2016). Entropy production in the flow over a swirling stretchable cylinder. *Thermophysics and Aeromechanics*, 23(3), 435–444. doi: 10.1134/S0869864316030136

[24] Osborne, M.R. (1969). On shooting methods for boundary value problems. *Journal of Mathematical Analysis and Applications*, 27(1). doi: 10.1137/0722018

[25] Das, K. (2013). Mixed convection stagnation point flow and heat transfer of Cu-water nanofluids towards a shrinking sheet. *Heat Transfer*, 42(3). doi: 10.1002/htj.21037

[26] Tie, P., Li, Q., & Xuan, Y. (2014). Heat transfer performance of Cu-water nanofluids in the jet arrays impingement cooling system. *International Journal of Thermal Sciences*, 77, 199–205. doi: 10.1016/j.ijthermalsci.2013.11.007